Pushing Heterojunction Technology Further: Novel Metallization Processes and Architectures

How novel SHJ applications are shaping the PV market

Nicola Frasson[1] [iD], and Marco Galiazzo[1] [iD]

[1] Applied Materials Italia srl, Italy

*Correspondence: Nicola Frasson, nicola_frasson@amat.com

Abstract. This work provides an overview on the different approaches to make Silicon Hetero-Junction cell (SHJ) production more scalable by investigating alternative metallization processes which can potentially be competitive with the standard Ag-based processes (Ag micro-size). With this purpose, this research aims at introducing the idea of widely using Ag-coated Cu formulations and/or low-Ag deposit solutions involving Ag nanoparticles-based formulations and reactive Ag (also referred as particle free) inks for both rear and front cell depositions on a single (finger and busbars) screen-printing process.

Keywords: Photovoltaics, Heterojunction, SHJ, Ag, Cu, AgCu, Nanoparticles, Metallization

1. Introduction

In the recent years, many ways have been explored in the attempt to decrease production costs, limit critical materials utilization and reduce Ag usage in the PV industry, targeting more sustainable manufacturing routes while also introducing new solar cell architectures that can provide electrical efficiencies that are superior to the current products on the market. Researchers are primarily investigating new solar cell and module metallization and interconnection strategies, introducing for Silicon Hetero-Junction (SHJ), TOPCon, Tandem and Back Contact (BC) solar cells and Ag-free or Ag-less metallization processes [1]. Market trends not only suggest that these technologies will get a larger share of the market in the next ten years but also tell us that more sustainable PV applications will be also largely integrated in buildings, vehicles, windows and more to face the energetic targets established with the Paris Agreement (deadline on 2050) [2] and deploy PV worldwide on very different surfaces and by using multiple integration methods [3], [4]. In this work, innovative solutions are presented mainly by considering newer metallization solutions that will reduce the cost of this manufacturing step. Most importantly, no dramatic changes in the equipment PV manufacturers will be needed to apply those concepts.

2. Materials and Methods

2.1 Materials

Previous experiments reported in literature [5] revealed a big potential in the use of SHJ solar cells as a viable route for a sustainable PV expansion because of the leaner production lines, low temperature processes, possibility to integrate non-standard paste formulations (for example, transparent conductive oxide layers can be an effective barrier for Cu migration into Si) and the potential to reach high conversion efficiency. It has been shown that the gap with the reference processes on standard SHJ substrates is still significant when these alternative materials are adopted (for example Cu based metallization had -0.8% average difference in cell efficiency with respect to Ag-based SHJ solar cells due to increased grid resistance). Moreover, reliability test failures for Cu based SHJ modules have been experienced at module level due to Cu oxidation (Thermal Cycling reduces the module power up to 40% in 200 cycles). Despite these early results, a huge interest in the evaluation of Nanoparticles (NPs) pure Cu ink (Cu), reactive Ag inks (Ag particle-free) and Ag-coated Cu particles (AgCu) is present, with the last process gaining an increased market share in the last quarters and being already introduced to production lines.

2.2 Methods

In our work we want to compare the different metallization pastes for screen-printing of SHJ cells by:

1. Sourcing alternative pastes with potential for metallization cost reduction
2. Developing a laboratory Best Known Method (BKM) for screen-printing standard Ag-based metallization (Ag micro-size) consisting in finding the proper printing parameters, screen type/mesh and overall process fine tuning.
3. Applying the BKM to the new materials (AgCu, Ag nano-size, Ag particle-free)
4. Comparing two different patterns for preliminary testing (test pattern) and actual production line simulation (full cell pattern)
5. Compare the different methods and results (line morphology inspection, IV testing, materials characterization)
6. Perform reliability testing on the most promising processes

The Ag production BKM will be used as a baseline for all the materials processing mentioned above and ad-hoc procedures will be then developed according to the materials properties and requirements in a second moment, like fine-tuning of the screen-printing parameters, screen design, thermal processes setup and more.

2.3 Materials characterization

Five pastes at different levels of readiness have been included in the analysis as reported below in Table 1 and Figure 1.

Table 1. Metallization pastes included in the analysis and their properties

PasteType	Ag ratio [%]	Curing Type [min, °C]	Storage [°C]	Viscosity @10 [1/s]	Thix. Index @1-10	Readiness Level
Ag micro-size	94	20, 200	4	76	13	Production
AgCu 1	44	20, 200	-10	64	11	Production
AgCu 2	55	20, 200	25	132	9	Prototype
Ag particle-free	33	20, 180	4	17	2.4	Prototype
Ag nano-size	>75	10, 200	25	73	18	Prototype

Figure 1. *Macroscopic appearance of the different materials; from the left: Ag micro, AgCu 1-2, Ag particle-free and Ag nano. Pastes differ in viscosity and color which is dependent on the particles size and shape (also coatings and ligands)*

Paste rheological properties have been studied using a reference procedure [6] named flow test (Figure 2) on our TA Instrument AR-2000 rheometer equipped with a plate-plate geometry and temperature control over the bottom plate (set at 25 °C, RT). This method provides information about the paste viscosity behaviour at increasing shear rate and it anticipates how the materials will perform once they are used for screen-printing applications.
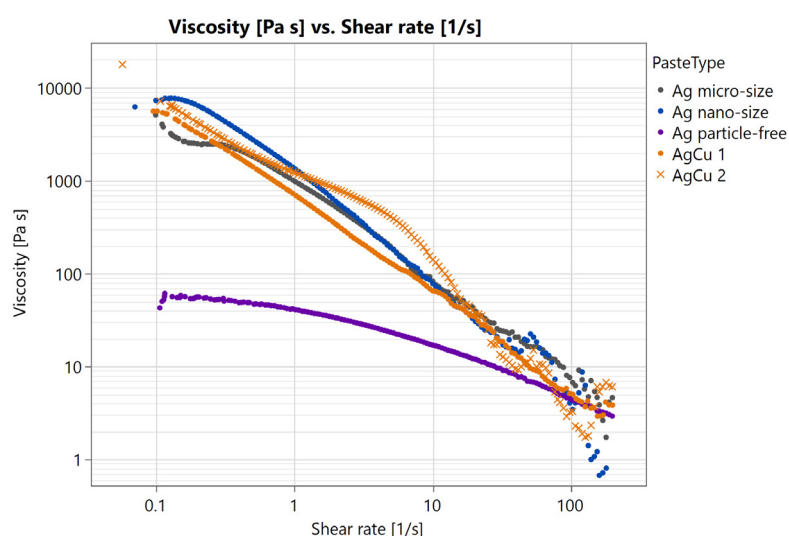
Figure 2. *Rheological properties of the different materials on the flow test*

Ag/AgCu nano and micro-size pastes have similar rheological properties (non-Newtonian pseudoplastic materials) while the Ag particle free ink has a very different viscosity trend at increasing shear rate, almost like a Newtonian fluid (viscosity in stable at increasing shear rate). According to the rheological properties, specific printing parameters have been used during the metallization process, suggesting quite different parameters to be necessary in some cases (mainly print speed, print force, flood speed and snap-off). In general, fast printing processes can be used (up 300 mm/s) while also limiting the Ag deposit and thus enabling several advantages,: 1) lower Ag consumption due to low Ag content in the paste, 2) less energetic curing process (shorter time and low temperature meaning a lower current consumption, e.g. nanoparticles are more reactive) and 3) lower sourcing and logistics costs (Cu is cheaper than Ag, some pastes can be also transported and stored at room temperature).

3. Results

3.1 Test pattern testing

Preliminary testing phases include the use of a test pattern screen (520/11 mesh, Polyamide emulsion, 10 µm Emulsion Over Mesh) which contains a range of screen openings spanning from 10 to 100 µm and including dog-bone patterns for line resistance measurements and consequent volume resistivity calculation (3 cm long lines with contacting pads at the ends, Figure 3).
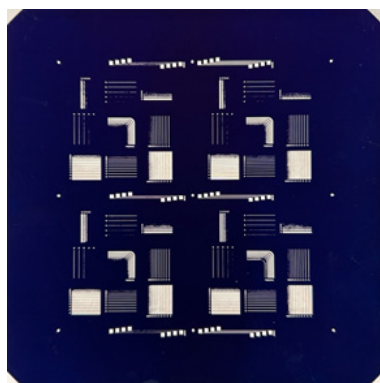
Figure 3. Test pattern print, thinner lines are not completely printed

The 30 and 50 µm wide screen openings have been used as a reference for both morphology investigations (30 µm) and electrical characterizations (50 µm). Also, similar printing parameters and the same drying and curing thermal processes have been used (50 mm/s print speed, 60 N/m, 1.5 mm snap-off; 30 s at 170° C drying process and 20 min at 200 °C curing process) for comparison (Table 2).

Table 2. Morphology and volume resistivity data measured on 50/300 reference lines

Paste Type	Line Width [µm]	Line Height [µm]	Ra – average roughness [µm]	Aspect Ratio	Vol. Res. [%]
Ag micro-size	44.4	7.3	2.5	0.16	Ref.
AgCu 1	42.0	8.5	2.3	0.20	+57%
AgCu 2	39.8	11.9	2.4	0.30	+45%
Ag part-free	55.1	0.6	0.4	0.01	+41%
Ag nano-size	46.7	9.6	1.9	0.20	+37%

All the line width measurements have been recorded by using a high-resolution microscope Microvu Vertex 420 while the height and roughness measurements come from a cell surface analysis performed on a Cyberscan Vantage profilometer.

Also, the Mitutoyo MF-U Series optical microscope on 20X optical zoom has been used for qualitative analysis and pictures recording (Figure 4).
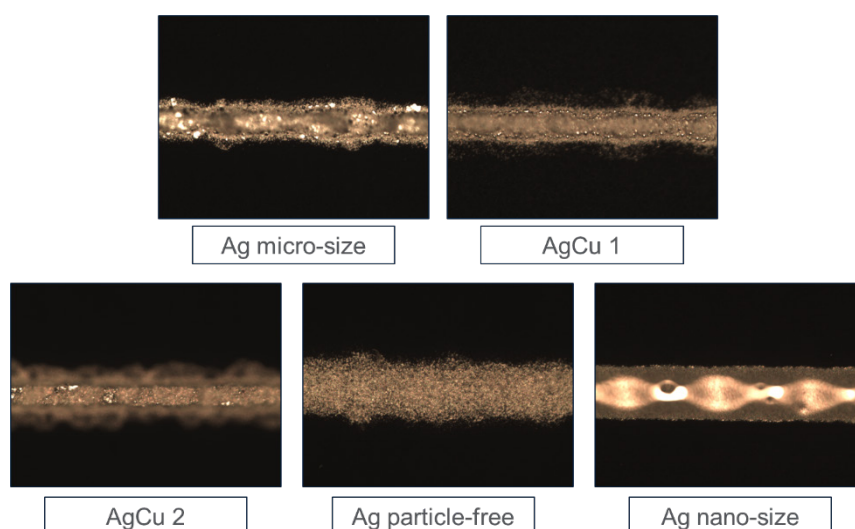
Figure 4. 30 µm screen opening printed lines after curing

This preliminary testing phase revealed the potential behind the alternative materials: 1) narrower or similar lines in terms of width (AgCu and Ag nano pastes), 2) high aspect ratio lines (all the pastes expect for Ag particle-free ink) and 3) lower roughness lines (Ag particle-free and Ag nano pastes) versus the reference. All these factors might contribute to similar-efficiency solar cells while limiting the Ag content, even if a higher amount of material will be required over the solar wafers to compensate the higher resistivity values than the reference Ag micro-size.

3.2 Full cell testing

After the preliminary testing, we printed a full pattern on finished SHJ M2 substrates (156.75 mm pseudo square wafer, 244.32 mm^2, 160 µm thick) as reported below on Table 3.

Table 3. Screens parameters; Back side screens were used first according to typical production line flows in which denser meshes and a higher finger (FF) density are used. Front side screens are in-stead thicker (larger wires, higher thickness) to allow a better aspect ratio of the FF that ideally have a rectangular shape (tall and thin). The choice of the busbars (BB) number depends on the solar simula-tor tool equipment and screens availability.

Side	Mesh	FF/BB (N)	FF opening [µm]
Front	380/14	74/6	38
Back	440/13	220/6	38

Unfortunately, only the AgCu 1 paste met the minimum print quality requirements and for this reason full cell data are only available for the process involving this material (Table 4, Figure 6). Typical failures reported for the remaining formulations include not complete transfer of the screen layout (mostly on cell edges, Figure 5), very slow printing speed needed (down to 50 mm/s) which are not acceptable in actual production conditions, paste spreading through the screen, not optimal paste flooding due to high stickiness of the paste leading at voids on the screen pattern and the use of the excessively high printing force over the screen to allow the paste transfer which can lead to screen breakages.

Figure 5. *Quality comparison on cell print; from the left: high and low printing quality cell (poor deposit on edges). Both the substrates are finished M2 textured SHJ wafers with TCO deposit on top (the blue color depends on the thickness of this last deposit)*

Most of the failures can be correlated with the rheological properties of the materials (viscosity values needs to stay in a specific range for proper print and flood phases) and their formulation additives and polymers can interact with the screen mesh and emulsion and cause cloggings in the screen openings, limiting of excluding the paste transfer especially on finger areas).

Table 4. *Printing parameters, deposits and IV results*

Process parameters and deposits (AMAT Tempo Presto™ printer)						
Paste	**Split**	**N**	**Speed [mm/s]**	**Cure [min]**	**Weight [mg]**	**Ag Cons. [mg/W]**
Ag-micro	Reference	11	100	20	246	46.4
AgCu 1	Split 10	5	200	10	233	19.3
	Split 20	5		20		
	Split 30	5		30		

Electrical-IV results (at 1000 W/m^2, AMAT Botticelli™ solar simulator)						
Paste	**Split**	**Eff. [%]**	**FF [%]**	**Rs [mOhm]**	**Isc [A]**	**Voc [mV]**
Ag-micro	Reference	21.95	79.91	2.05	9.23	726
AgCu 1	Split 10	21.87	79.77	2.45	9.22	726
	Split 20	21.94	79.77	2.38	9.24	727
	Split 30	21.87	79.72	2.52	9.23	725
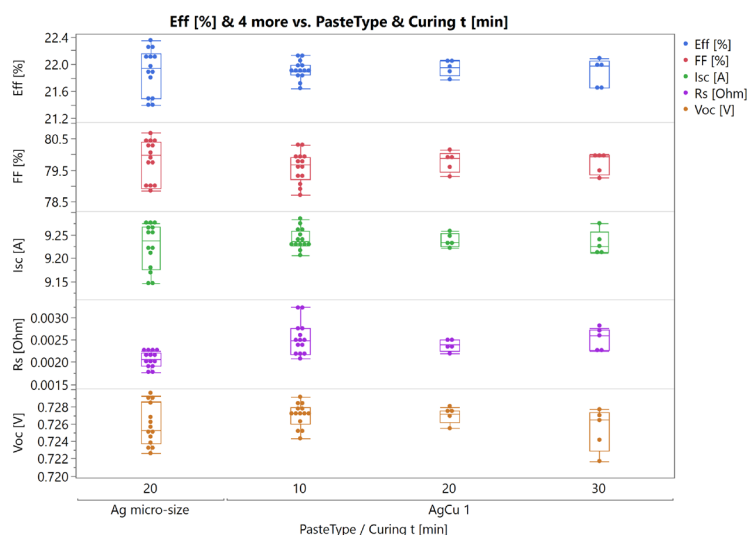
Figure 6. *IV results for reference and AgCu 1 pastes*

All the cells went through the same thermal treatment conditions meaning the same drying process to remove the organic solvents (30 s at 170° C on a belt oven, infrared lamps exposure and hot-air flow) and curing process for metal sintering (box-static oven at 200° C, different curing times are reported in the Table 4 so providing three different cells splits). All the electrical/IV data have been recorded by using Applied Materials Botticelli™ solar simulator tool equipped with a LED multi-spectral source and properly calibrated with a reference cell. AgCu1 and the reference process are not significantly different in terms on Eff, FF, Rs and Isc values. Also, the process comparison is fair since the SHJ wafers have been selected among the different batches by keeping the same average Voc value. However, the higher Rs in the AgCu 1 process led to a lower FF and Eff which is mainly due to the intrinsic properties of the material.

When evaluating the Ag Consumption per Watt metric on M2 SHJ cells produced it is evident that the values reported in Table 4 are representative of a laboratory scale test and valid for comparative tests, due to the hardware limitations, screens layout and work environment. Customer production data on G12 SHJ (210 mm pseudo square wafers, 440.96 mm^2) shown an average Ag consumption of 25.7 mg/W, meaning 10 mg/W when using AgCu potentially by applying the learning curve we experimented at lab scale. These data provide a very important insight on the AgCu adoption trend, showing the impact of implementing these novel materials at production scale and so limiting the Ag consumption and make the 1TW/y cells production sustainable by using SHJ cells as primary source of energy (Figure 7) [7]. Furthermore, the AgCu 1 paste seems promising also in terms of curing processes, allowing the use of much shorter curing times down to 10 minutes so decreasing the energy consumption along the production process.
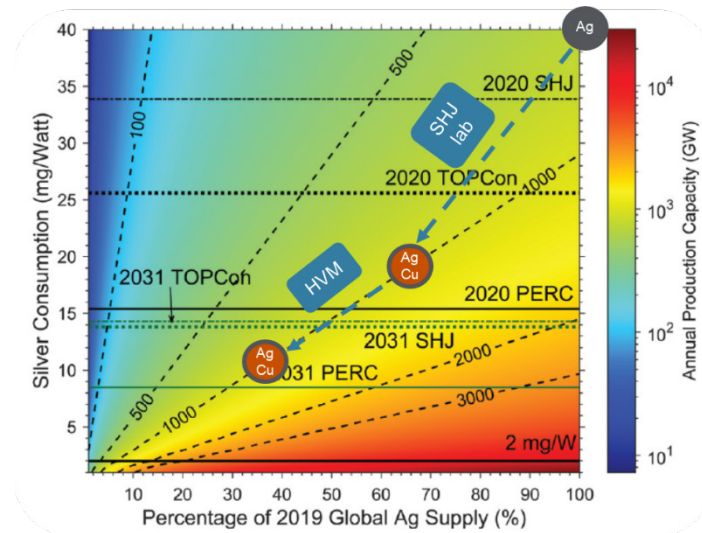
Figure 7. *Ag consumption and production capacity over global Ag supply [7]. AgCu scalability added to the original graph (blue and orange shapes). Dashed lines represent the annual production capacity (GW), 1 TW is considered as a reference for the roadmap*

Below are reported the EL images of the most efficient cells for the two batches (Figure 8), showing a uniform infrared emission all over the two solar cells, indicating a uniform cell deposit and no high-resistance area. Dark areas are mainly related to SHJ substrate defects.
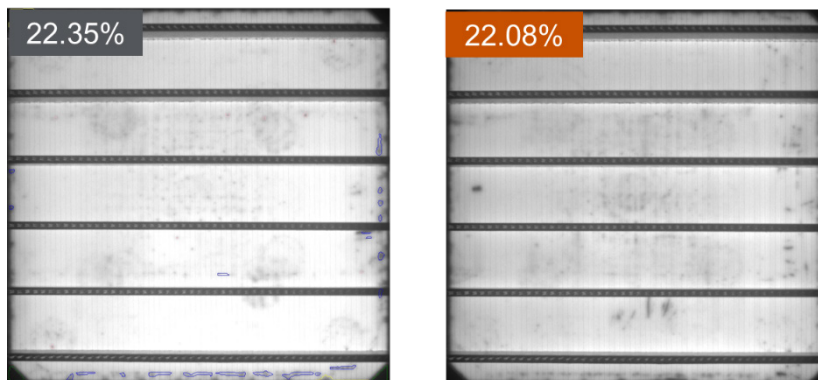
Figure 8. *EL images; from the left: Ag cell and AgCu 1 cell*

Finally, a Scanning Electron Microscopy (Hitachi TM-3000 SEM) inspection was also performed on the solar cells (Figure 9). This analysis was useful in providing more information about the paste morphology at sub-micron level, showing how particles are sintering and aggregating during and after the screen-printing phase. Furthermore, the energy dispersive X-ray analysis (EDX) gave a quantitative evaluation of the elements exposed over the paste surface (Table 5).
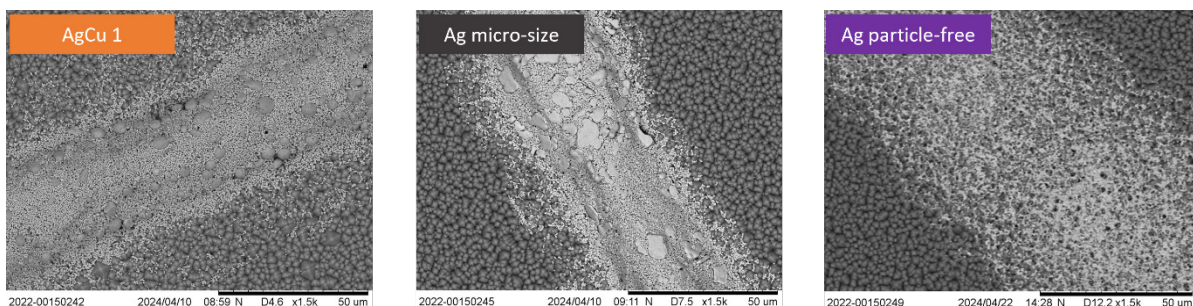
Figure 9. *SEM inspection over AgCu, Ag and Ag particle-free samples, 1500X zoom*

Note that in the AgCu 1 case, the average spherical aggregates size is around 4.9 μm while in the Ag micro-size case the aggregates have a flake-shape and an average size of 8.4 um (almost double).

Table 5. EDX analysis results, 3000X (particle free) and 5000X (Ag and AgCu) zoom

Elements	AgCu 1	Ag micro-size	Ag particle-free
Cu	0.3	0	0
Ag	18.8	12.6	18.2
Tantalum	21.1	50.2	25.6

From EDX, only a limited amount of exposed Cu is detected, meaning that the core-shell nanoparticles structure is stable along the process. The Ag micro-size paste is used to normalize eventual Cu contamination of the production lines. Also, the SEM analysis highlighted that the Ag particles are very dispersed when using the particle free ink, partly explaining the higher volume resistivity with respect to the reference paste: depositing more paste (double-print, different print parameters and/or viscosity adjustments) may improve the metallization results.

As a conclusion, the slightly lower efficiency on the AgCu 1 paste than the reference process seems mostly related to the intrinsic properties of the materials than the screen-printing process itself.

3.3 Temperature stability testing

Cu oxidation depends on environmental conditions such as oxygen, temperature and humidity. Researchers are investigating ways to integrate pure Cu as a dramatic solution to solve the Ag consumption issue, [8] but oxidation-related issues and reliability failures (damp-heat or thermal cycles) are still limiting factors. In this case, Cu is part of a core-shell structure in which the core of the particle is made by the Cu itself and the external shell is made by a few nanometers of Ag [9], [10], [11]. This setup prevents Cu surface from oxidation and limits the impact on the cell's efficiency by keeping the series resistance values stable at increasing temperatures. This provides a first step further in Cu-Ag pastes integration at single-cell level and do not provide a final response on the complete integration at module level [12], in accordance with IEC 61215.

To evaluate this, the temperature stability testing is a crucial part in the materials evaluation to finally check whether a paste can be fully integrated on a production line, from screen-printing to cell-to-module interconnection, or not. As part of this evaluation, data from previous work from the our team [5] have been also included to show the impact of a core-shell structure in maintaining Cu stable at increasing temperatures (Figure 10). In accordance with the previous tests, we heated several bare cells per batch on a drying box oven for 10 mins at three different temperatures in air and performed IV tests before and after the heating by using a solar simulator (standard cell measurement, BB contact and 1000 W/m^2 exposure). Ag micro-size paste has been also used as a reference.
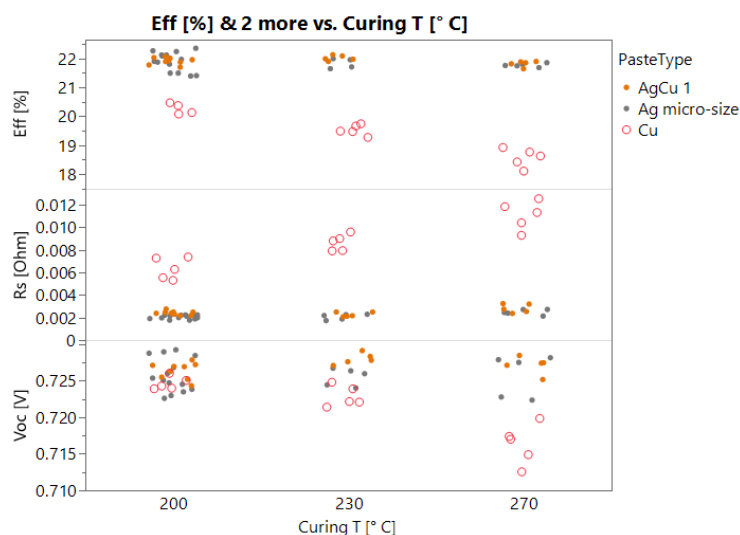
Figure 10. *Efficiency, series resistance and open circuit voltage values at increasing temperatures for paste reliability comparison*

For pure-copper pastes, the drop in cell efficiency is very clear and the main reason is oxidation (this is clearly visible by looking at the cells, printed lines appear of blue-green colors). Standard Ag and AgCu pastes instead show a good resilience and tolerance to high temperatures which is almost the same (Table 6), just a few mOhm gain in series resistance for every temperature range we have considered (series resistance gains are mostly related to oxidations as well). Therefore, the overall efficiency of the solar cell will be dramatically impacted because of the high correlation between series resistance and efficiency.

Table 6. *Reliability testing results focusing on series resistance values variations on single solar cells*

PasteType	∆Rs 200-230 [mOhm]	∆Rs 230-270 [mOhm]
Ag micro-size	+0.2	+0.4
AgCu 1	+0.1	+0.5
Cu	+2.3	+2.4

4. Conclusions

In this work, the potential of alternative metallization pastes for screen printing of SHJ cells is presented. Although most of the above materials are still under development, preliminary characterizations have shown they could provide superior print morphology (narrower and taller lines) with reduced Ag consumption. AgCu 1 paste, with Cu core and Ag coated particles, seems to be a valid alternative to pure Ag paste by matching the electrical and temperature stability performance of the reference Ag. This would enable the introduction of Cu metallization on SHJ without obvious metal oxidation or migration. In parallel with screen-printing, we plan to evaluate alternative deposition techniques for reference and alternative materials, with a special focus on parallel dispensing [13]: this methodology allows an extremely uniform finger deposit, meaning better profiles, reducing the line resistance and increasing the cell efficiency.

Data availability statement

Raw data in this paper are under restricted diffusion and NDAs (third-party data, legal or ethical constraints) and will not be publicly available. Please contact the corresponding authors for further information and disclosures.

Author contributions

Competing interests

Funding

Acknowledgement

References

[1] ITRPV 2023, p. 30, 2023.

[2] PJ., Verlinden et al., "Future challenges for photovoltaic manufacturing at the terawatt level" Journal of Renewable Sustainable Energy, vol. 12, p. 053505, 2020. DOI: 10.1063/5.0020380

[3] S., Harrison et al., Photovoltaics International, "Pushing the limits of shingle heterojunction module performance, cost and sustainability", vol. 49, pp. 48-58, 2023.

[4] M., Foti et al., "22% efficiency module combining Silicon Heterojunction Solar and Shingle interconnection", 49th PSVC, 2022. DOI: 10.1109/PVSC48317.2022.9938591

[5] N., Frasson et al., "Evaluation of different approaches for HJT cells metallization based on low temperature Ag pastes", EU PVSEC Proc., pp. 162-166, 2021. DOI: 10.4229/EUPVSEC20212021-2BO.14.6

[6] S., Thibert et al., "Influence of silver paste rheology and screen parameters on the front side metallization of silicon solar cell", Materials Science in Semiconductor Processing, pp. 790-799, 2014. DOI: 10.1016/j.mssp.2014.08.023

[7] Y., Zhang et al., "Design considerations for multi-terawatt scale manufacturing of existing and future photovoltaic technologies: challenges and opportunities related to silver, indium and bismuth consumption", Energy and Environmental Science, vol. 14, p. 5587, 2021. DOI: 10.1039/D1EE01814K

[8] N., Chen et al., "Thermal Stable High-Efficiency Copper Screen Printed Back Contact Solar Cells", Solar RRL, vol. 7, no. 2, p. 2200874, 2022. DOI: 10.1002/solr.202200874

[9] J., Schube et al., "Advanced metallization with low silver consumption for silicon heterojunction solar cells", AIP Conf. Proc. 2156, vol. 2156, no. 1, p. 020007, 2019. DOI: 10.1063/1.5125872

[10] M., Grouchko et al., "Formation of air-stable copper–silver core–shell nanoparticles for inkjet printing", Journal of Materials Chemistry, vol. 19, pp. 3057-3062, 2009. DOI: 10.1039/b821327e

[11] S., Jongmin et al., "Synthesis of Silver-coated Copper Particles with Thermal Oxidation Stability for a Solar Cell Conductive Paste", Chemistry Letters, vol. 44, no. 9, pp. 1223-1225, 2015. DOI: 10.1246/cl.150424

[12] M., Aghaei et al., "Review of degradation and failure phenomena in photovoltaic modules", Renewable and Sustainable Energy Reviews, vol. 159, p. 112160, 2022. DOI: 10.1016/j.rser.2022.112160

[13] Si., Pordan et al., "Optimizing solar cell metallization by parallel dispensing", Solar Energy Materials and Solar Cells, vol. 266, p. 112685, 2024. DOI: 10.1016/j.solmat.2023.112685